J Appl Electrochem (2008) 38:279–287
DOI 10.1007/s10800-007-9436-8

ORIGINAL PAPER

Corrosion inhibition of mild steel in acidic medium using hydrazide derivatives

A. V. Shanbhag · T. V. Venkatesha · R. A. Prabhu · R. G. Kalkhambkar · G. M. Kulkarni

Received: 11 July 2007 / Revised: 1 October 2007 / Accepted: 15 October 2007 / Published online: 6 November 2007

Abstract The corrosion inhibition characteristics of *N*′-[(1E)-(4-hydroxy phenyl) methylene] isonicotinohydrazide (HIH) & *N*′-[(1E)-(4-hydroxyl-3-methoxy phenyl) methylene] isonicotinohydrazide (HMIH) on mild steel corrosion in 1 M hydrochloric acid were investigated by weight loss, potentiodynamic polarization and impedance techniques. The inhibition efficiency increased with increase in inhibitor concentration but decreased with increase in temperature. The thermodynamic functions of dissolution and adsorption processes were evaluated. The polarization measurements indicated that the inhibitors are of mixed type. The adsorption of the compounds was found to obey Langmuir's adsorption isotherm. Passive film characterization was done by Fourier transform infrared (FTIR) spectra and scanning electron microscopy (SEM).

Keywords Corrosion inhibition · Adsorption isotherm · Mild steel · Thermodynamic parameters · Hydrazides

A. V. Shanbhag
Department of Chemistry, S.D.M. College, Honavar 581 334, Karnataka, India

T. V. Venkatesha (✉)
Department of P.G. Studies and Research in Chemistry, Kuvempu University, Shankarghatta 577 451, Karnataka, India
e-mail: drtvvenkatesha@yahoo.co.uk

R. A. Prabhu
Department of Chemistry, M.G.C. College, Siddapur 581 355, Karnataka, India

R. G. Kalkhambkar · G. M. Kulkarni
Department of Chemistry, Karnatak Science College, Dharwad, Karnataka, India

1 Introduction

Chloride, sulphate and nitrate ions in aqueous media are particularly aggressive to mild steel and accelerate its corrosion. The service life of steel is enhanced by various corrosion control methods based on modifying either the surface of the metal or the local environment to which the metal is exposed. Corrosion of steel is effectively controlled by the application of suitable inhibitors [1]. The majority of the well-known corrosion inhibitors are compounds containing nitrogen, oxygen, phosphorus and sulphur in their functional groups with aromatic and heterocyclic rings [2–11]. Most of these organic compounds are adsorbed on the metal surface and provide a barrier between metal and environment, thereby reducing the rate of corrosion. The effectiveness of inhibition depends on the nature and surface charge of the metal, the nature of the medium, the nature and chemical structure of the inhibitor molecule such as functional groups, aromaticity, the π orbital character of the donating electron, steric factor, and electron density at the donor atoms [12–15].

Many corrosion inhibitors used in aqueous heating and cooling systems are generally toxic and generate health hazards [16]. This toxic property limits the field of their applications. However there is a great demand for non-toxic corrosion inhibitors. Hydrazide derivatives investigated in the present work are non-toxic in nature [17–19]. Further these are heterocyclic compounds containing benzene and pyridine rings connected through amide carbonyl and imine groups. The electron density on these groups is enhanced due to the presence of hydroxyl and methoxy groups of the benzene ring. This may lead to a better interaction with the metal.

This paper describes a study of corrosion inhibition characteristics of *N*′-[(1E)-(4-hydroxy phenyl) methylene]

isonicotinohydrazide (HIH) & *N′*-[(1E)-(4-hydroxyl-3-methoxy phenyl) methylene] isonicotinohydrazide (HMIH) on mild steel corrosion in 1 M HCl. The behaviour has been investigated and inhibition efficiency has been determined by chemical (weight loss) and electrochemical (potentiodynamic polarization and impedance) methods. It is also aimed at predicting the thermodynamic feasibility of adsorption of the inhibitor molecules on steel and to study their adsorption behaviour.

2 Experimental details

2.1 Materials

Mild steel of composition C = 0.05%, Mn = 0.35%, P = 0.032%, S = 0.033%, the remainder being Fe, was used for all experiments. Rectangular mild steel specimens of size 5 × 1 × 0.1 cm were used. The samples were mechanically polished with different grades of emery papers, degreased with trichloro ethylene, washed with triply distilled water and finally dried. AR grade chemicals and triply distilled water were used in the preparation of the test solutions.

The inhibitors employed were the condensation products of the reaction between *p*-hydroxy benzaldehyde and *p*-vanillin with isonicotinic acid hydrazide. A mixture of *para* hydroxyl benzaldehyde (0.02 mol) + isonic azide (0.02 mol) and a mixture of *para* vanillin (0.02 mol) + isonic azide (0.02 mol) were separately taken in 20 cm^3 of ethanol containing 1 cm^3 of acetic acid, stirred well for 4 h. The solids separated were filtered off and crystallized from ethanol. The concentration range of inhibitors employed was 1.56–25 × 10^{-5} M.

The chemical structures of compounds are given in Fig. 1. Spectroscopy characterization of the compounds is given below

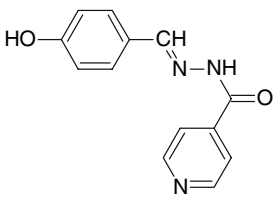

N'-[(1*E*)-(4-hydroxyphenyl)methylene]isonicotinohydrazide **(HIH)**

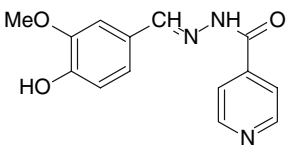

N'-[(1*E*)-(4-hydroxy-3-methoxyphenyl)methylene]isonicotinohydrazide **(HMIH)**

Fig. 1 Chemical structures of inhibitors

1. Schiff base derived from *p*-hydroxy benzaldehyde (HIH)
I.R (KBr, Cm^{-1}): 1620 (N=C), 1660 (NHC=O), 3240 (OH), 3360 (NH)
^{1}H NMR (δ ppm, $CDCl_3$): 6.84–8.30 (m, 8H, Ar–H), 7,20 (s, 1H, =CH), 11.60 (s, 1H, NH), 12,10 (s, 1H, OH)
FAB-MS: *m/z* 242 (M + H)
2. Schiff base derived from *p*-vanillin (HMIH)
I.R (KBr, Cm^{-1}): 1630 (N=C), 1669 (NHC=O), 3220 (OH), 3330 (NH)
^{1}H NMR (δ ppm, $CDCl_3$): 3.80 (s, 3H, OCH_3), 6.80–8.20 (m, 8H, Ar–H), 7,30 (s, 1H, =CH), 11.40 (s, 1H, NH), 12,20 (s, 1H, OH)
FAB-MS: *m/z* 272 (M + H)

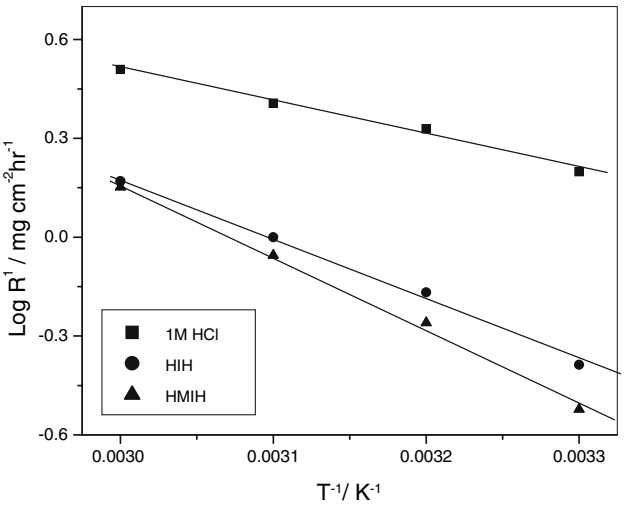

Arrhenius plots of corrosion rates with temperature in the presence and absence of inhibitor

2.2 Weight loss studies

Weight loss measurements were carried out by weighing the cleaned and dried mild steel specimens before and after immersion in acid solutions for 4 h in the absence and presence of various concentrations of HIH and HMIH. Runs were also done at different temperatures (303, 313, 323 & 333 K). Duplicate experiments were performed in each case and the mean value of the weight loss was noted. Corrosion rate (R^1in mg cm^{-2} h^{-1}) and Inhibition efficiency (IE%) were calculated.

2.3 Potentiodynamic polarization studies

The potentiodynamic polarization studies were carried out with mild steel strips having an exposed area of 1 cm^2. A

conventional three electrode cell consisting of mild steel as working electrode, Platinum foil as counter electrode and a Saturated Calomel Electrode as reference was used. Potentiodynamic polarization studies were carried out using an Autolab Potentiostat–Galvanostat and the data was analysed using GPES software. In the case of polarization measurements, the potential sweep rate was 2 mV s^{-1}. The inhibition efficiencies were calculated from corrosion currents determined using the Tafel extrapolation method.

2.4 Electrochemical impedance studies

Electrochemical impedance measurements were carried out using an electrochemical system Frequency Response Analyser (FRA). The electrochemical impedance spectra (EIS) were acquired in the frequency range 10 kHz to 10 mHz at the rest potential by applying 5 mV sine wave AC voltage. The double layer capacitance (C_{dl}) and the polarization resistance (R_p) were determined from Nyquist plots [20]. The inhibition efficiencies were calculated from R_p values.

2.5 Fourier transform infrared (FTIR) spectroscopic studies

The mild steel specimens were immersed in various test solutions for a period of 24 h. After 24 h, the specimens were taken out and dried. The surface film was scratched carefully and its FTIR spectra were recorded using Nicolet Avtar 330 FT–IR instrument.

2.6 Scanning electron microscopic studies

After immersion the steel specimens were removed and dried. The specimens were coated with film of 50 nm of gold by sputtering and investigated using a JEOL JSM—840A scanning electron microscope. The energy of the accelerating beam employed was 20 kV.

3 Results and discussion

3.1 Weight loss measurements

Table 1 shows the corrosion rate (R^1) and IE (%) for varying concentrations of HIH and HMIH in 1 M HCl solution at 303 K. The weight loss decreased and the inhibition efficiency increased with increasing additive concentration for both compounds. However, HMIH showed better IE than HIH. The highest inhibition efficiency of 81% was observed with HMIH at 25×10^{-5} mol dm^{-3} concentration. The inhibition efficiencies did not change at higher additive concentration than 25×10^{-5} mol dm^{-3}.

Table 1 Corrosion parameters obtained from weight loss measurements in 1 M HCl containing different concentrations of inhibitor at 303 K

Inhibitor	Concentration ($10^5 \times$ M)	Weight loss (mg)	Corrosion rate (mg cm^{-2} h^{-1})	Inhibition efficiency (%)
–	0	63	1.58	–
HIH	1.56	37.8	0.95	40
	3.13	30.2	0.76	52
	6.25	24.6	0.61	61
	12.50	19.5	0.49	69
	25.00	16.4	0.41	74
HMIH	1.56	35.9	0.90	43
	3.13	27.7	0.69	56
	6.25	18.9	0.47	70
	12.50	15.8	0.39	75
	25.00	12.0	0.30	81

3.2 Effect of temperature

The values of corrosion rate and inhibition efficiency of HIH and HMIH at 25×10^{-5} mol dm^{-3} concentration at different temperatures are given in Table 2. The inhibition efficiency decreased with increase in temperature from 303 to 333 K. This indicates desorption of inhibitor molecules from the metal surface. The value of activation energy (E_a) was calculated from the slope of the straight line obtained by plotting log $R^1_.$ versus $1/T$ according to the Arrhenius equation

$$R^1_. = A\exp(-E_a/RT) \quad (1)$$

It was found that E_a values for inhibited systems were higher than for the uninhibited system (Table 2). Due to this increase in the activation energy the dissolution decreased. However with increase in temperature there was an appreciable decrease in the adsorption of the inhibitors on the metal surface and a corresponding rise in the corrosion rate occurred [21].

Equations 2 and 3 were used to calculate the thermodynamic parameters [22] for the adsorption process:

$$\Delta G^0_{ads} = -2.303RT \log 55.5K \quad (2)$$

where K is given by

$$K = \frac{\theta}{C_{inh}(1-\theta)} \quad (3)$$

where θ is the degree of coverage on the metal surface, C is the concentration of inhibitor in mol dm^{-3} and K is the equilibrium constant for adsorption process. The average

Table 2 Corrosion parameters obtained from weight loss measurements at different temperatures in 1 M HCl containing 25 × 10^{-5} mol dm^{-3} of inhibitors (Wt. loss in mg and R^1 in mg cm^{-2} h^{-1})

Temperature (K)	1 M HCl		HIH			HMIH		
	Wt. loss	R^1	Wt. loss	R^1	IE%	Wt. Loss	R^1	IE%
303	63	1.58	16.4	0.41	74	12.0	0.30	81
313	85	2.13	27.2	0.68	68	22.1	0.55	74
323	102	2.55	39.8	1.00	61	35.7	0.89	65
333	129	3.23	59.3	1.48	54	56.8	1.42	56
E_a (kJ)	19.92	19.92	38.3	38.3	38.3	43.78	43.78	43.78

thermodynamic parameter, enthalpy of adsorption (ΔH^0_{ads}) and ΔS^0_{ads} were obtained from the plot of log K versus $1/T$ (Fig. 2) using the equation

$$\log K = \frac{1}{2.303}\left(-\frac{\Delta H^0_{ads}}{RT} + \frac{\Delta S^0_{ads}}{R}\right) \quad (4)$$

The calculated values of K, ΔH^0_{ads}, ΔG^0_{ads} and ΔS^0_{ads} over the temperature range 303–333 K are recorded in Table 3. The negative value of ΔG^0_{ads} and positive value of ΔS^0_{ads} indicate the spon6taneous adsorption of inhibitor on the surface of mild steel [23, 24].

3.3 Polarization studies

Polarization curves for steel in 1 M HCl in the absence and presence of HIH and HMIH at 303 K are shown in Figs. 3 and 4. In both the cases, the addition of the compounds reduced both anodic and cathodic currents. Various corrosion parameters such as corrosion current density (I_{corr}), Tafel slope constants (b_a & b_c), corrosion potential (E_{corr}), corrosion rate, IE (%) and surface coverage degrees (θ) are given in Table 4. These results show that the compounds act as effective inhibitors. Corrosion inhibition increases with inhibitor concentration. The variation in inhibition action depends on the type and nature of the inhibitor molecule. The protection action can be attributed to the electron density of the azomethine (–C=N–) group and this electron density varies with the substituents in the inhibitor molecule. The OH group, being electron donating, and the isonicotinic acid hydrazide, being electron withdrawing, the electron movement within the molecule is more facile. The imine nitrogen can donate the lone pair of electrons to the metal surface to adsorb more easily and hence reduce the rate of corrosion [25]. The IE of HMIH was higher than HIH, which can probably be explained by the presence of one more electron donating methoxy group in the molecule [26]. The corrosion potential (E_{corr}) was almost constant with additive concentration. It is obvious from the polarization curves that both anodic as well as cathodic curves shift towards lower current density with the concentration of inhibitors. It was further noticed that both anodic and cathodic polarization profiles are influenced simultaneously, almost to the same extent, suggesting the mixed action of the inhibitors [25].

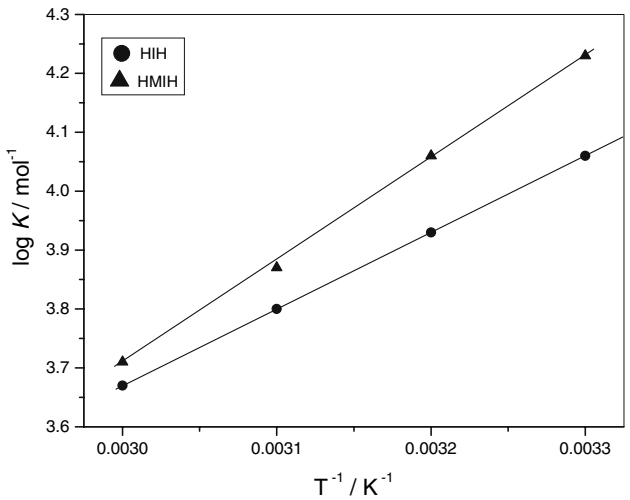

Fig. 2 Plot of log K against $1/T$ for HIH and HMIH derived from experimental adsorption for mild steel at different temperatures

3.4 Adsorption isotherms

The degree of surface coverage (θ) was determined by IE%. The plots of log ($\theta/1-\theta$) versus log C were linear (Fig. 5) indicating Langmuir adsorption. The adsorption of HIH and HMIH molecules formed a barrier, which prevented the contact of metal with electrolyte. Hence the corrosion rate was reduced.

3.5 Spectral studies

FTIR spectra were recorded to understand the interaction of inhibitor molecules with the metal surface. Figures 6a

Table 3 Thermodynamic parameters for the adsorption of inhibitors in 1 M HCl on mild steel

Inhibitor	Temperature (K)	$-\Delta H^0_{ads}$ (kJ mol^{-1})	$10^{-3} \times K$ (mol^{-1})	$-\Delta G^0_{ads}$ (kJ mol^{-1})	ΔS^0_{ads} (J mol^{-1})
HIH	303	24.6	11.4	40.2	68
	313		8.5		
	323		6.3		
	333		4.7		
HMIH	303	33.5	17.1	40.8	67.8
	313		11.4		
	323		7.4		
	333		5.1		

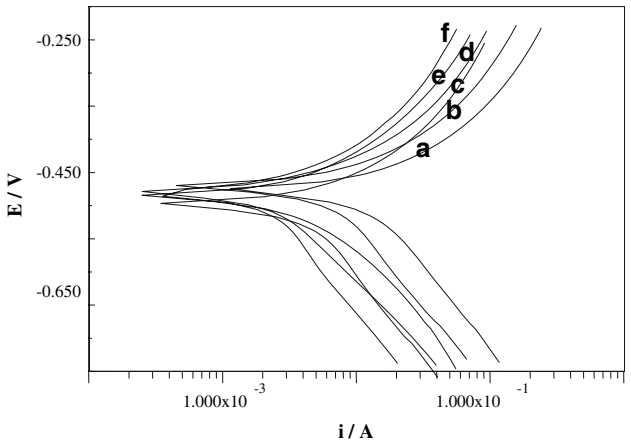

Fig. 3 Polarization curves of mild steel in 1 M HCl in the presence of different concentrations of HIH at 303 K (**a**) Blank (**b**) 1.56×10^{-5} M (**c**) 3.125×10^{-5} M (**d**) 6.25×10^{-5} M (**e**) 12.5×10^{-5} M (**f**) 25×10^{-5} M

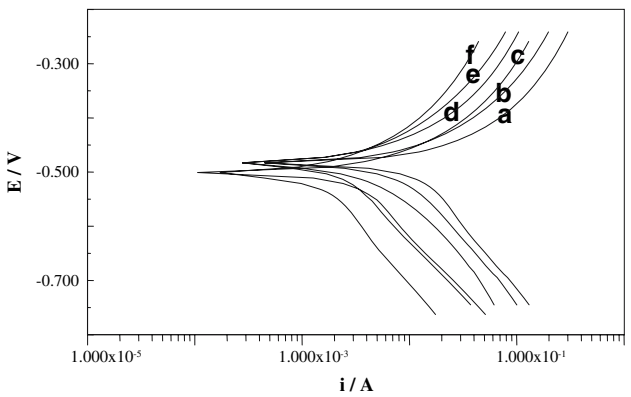

Fig. 4 Polarization curves of mild steel in 1 M HCl in the presence of different concentrations of HMIH at 303 K. (**a**) Blank (**b**) 1.56×10^{-5} M (**c**) 3.125×10^{-5} M (**d**) 6.25×10^{-5} M (**e**) 12.5×10^{-5} M (**f**) 25×10^{-5} M

and 7a show the IR spectra of pure hydrazides HIH and HMIH and Figures 6b and 7b represent the spectra of the scraped samples obtained from the metal surfaces after corrosion experiments. Several peaks in the spectrum of pure compounds were modified in the spectrum of scraped samples. The involvement of imino nitrogen in the electron pair donation to the metal surface can be depicted as shown in Fig. 8.

This is by changes in the stretching frequencies of the amide carbonyl observed at 1,647 cm^{-1} (HIH) and 1,659 cm^{-1} (HMIH) in the pure compounds and due to binding with metal as shown in the Fig. 8. The stretching frequency of the amide carbonyl in both the inhibitors were observed at lower frequencies of 1,629 and 1,639 cm^{-1}, respectively.

3.6 Electrochemical impedance spectroscopy (EIS)

The results can be interpreted in terms of the equivalent circuit of the double layer shown in Fig. 9, which has been used previously to model the iron–acid interface [27].

The corrosion behaviour of mild steel in acid solution in the presence of hydrazide derivatives was investigated by EIS at room temperature. Figures 10 and 11 show a typical set of Nyquist plots for mild steel in 1 M HCl in the absence and presence of HIH and HMIH at various concentrations. The impedance response of mild steel in uninhibited HCl is significantly changed after addition of hydrazide derivatives to the corrosive media. The semicircle radii depend on the additive concentration. The diameter of the capacitive loop increased with increasing concentration, the increase in HMIH being higher. R_p is inversely proportional to the corrosion current and was used to calculate the inhibition efficiency from Eq. 5 [28]

$$\mathrm{IE}\% = \frac{R_{p,i} - R'_{p,o}}{R_{p,i}} \times 100 \quad (5)$$

where, $R_{p,i}$ and $R'_{p,o}$ are the polarization resistances with and without the additives, respectively.

Table 4 Corrosion parameters obtained from polarization measurements for mild steel in 1 M HCl containing various concentrations of inhibitors at 303 K

Inhibitor	Concentration ($M \times 10^5$)	$-E_{corr}$ (V)	$10^3 \times I_{corr}$ (A cm^{-2})	θ	b_a ($Vdec^{-1}$)	b_c ($Vdec^{-1}$)	R^1 (mm $year^{-1}$)	IE (%)
–	0	0.482	6.43	–	0.146	0.268	77.7	–
HIH	1.56	0.482	3.99	0.38	0.135	0.206	48.2	38
	3.13	0.488	3.35	0.48	0.141	0.169	40.4	48
	6.25	0.494	2.86	0.56	0.126	0.239	34.5	56
	12.50	0.490	2.39	0.63	0.122	0.212	28.8	63
	25.00	0.482	1.78	0.72	0.109	0.132	21.6	72
HMIH	1.56	0.489	3.74	0.42	0.129	0.221	37.2	42
	3.13	0.487	3.09	0.52	0.120	0.195	37.3	52
	6.25	0.483	2.73	0.58	0.131	0.204	33	58
	12.50	0.494	1.76	0.73	0.103	0.204	21.2	73
	25.00	0.497	1.51	0.77	0.115	0.185	18.3	77

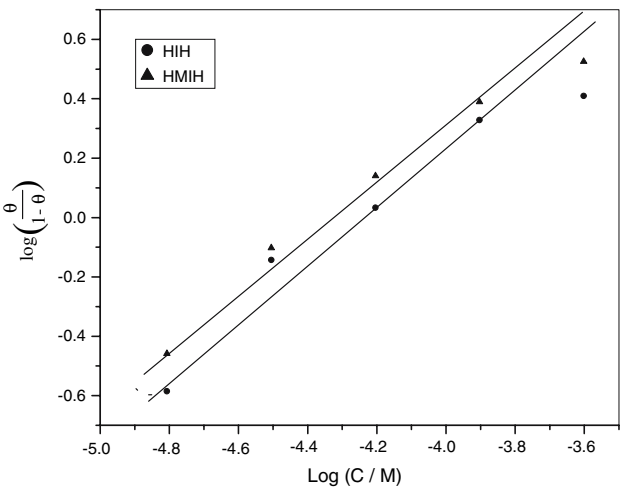

Fig. 5 Langmuir adsorption isotherm for mild steel in 1 M HCl containing various concentrations of inhibitor from polarization study

Impedance parameters for mild steel in 1 M HCl with and without inhibitors are given in Table 5. The R_p & IE% values increased with additive concentration and the capacitance values (CPE) decreased, indicating the formation of a surface film [29]. R_p values obtained with HMIH were greater than HIH indicating higher inhibiting action of HMIH.

3.7 SEM studies

To demonstrate the presence of an organic film on the steel specimens, scanning electron microscopic images were recorded. Figure 12a shows the scanning electron microscopy (SEM) image of corroded steel in 1 M HCl. The surface is covered with a high density of pits. Figure 12b

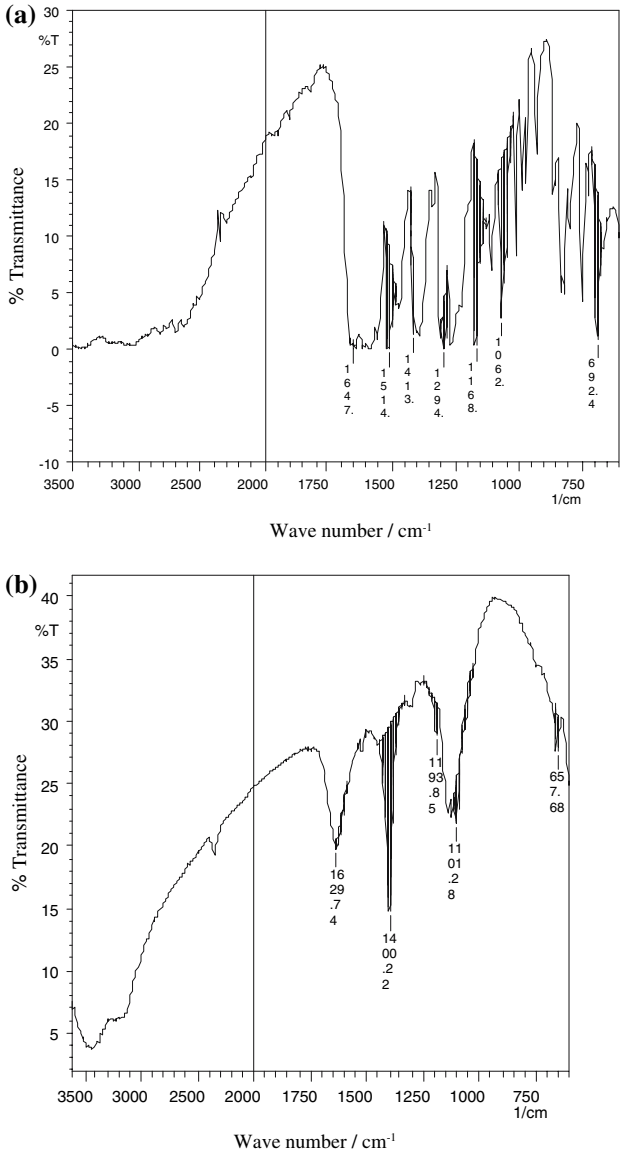

Fig. 6 (**a**) IR Spectra of HIH. (**b**) IR Spectra of scraped sample (HIH)

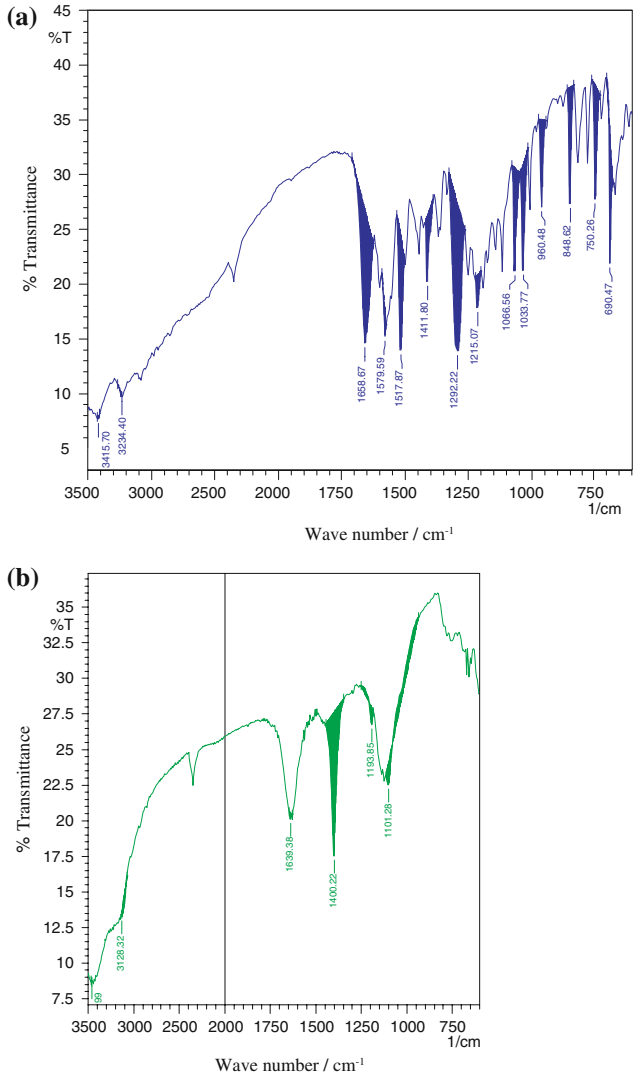

Fig. 7 (**a**) IR Spectra of HMIH. (**b**) IR Spectra of scraped sample (HMIH)

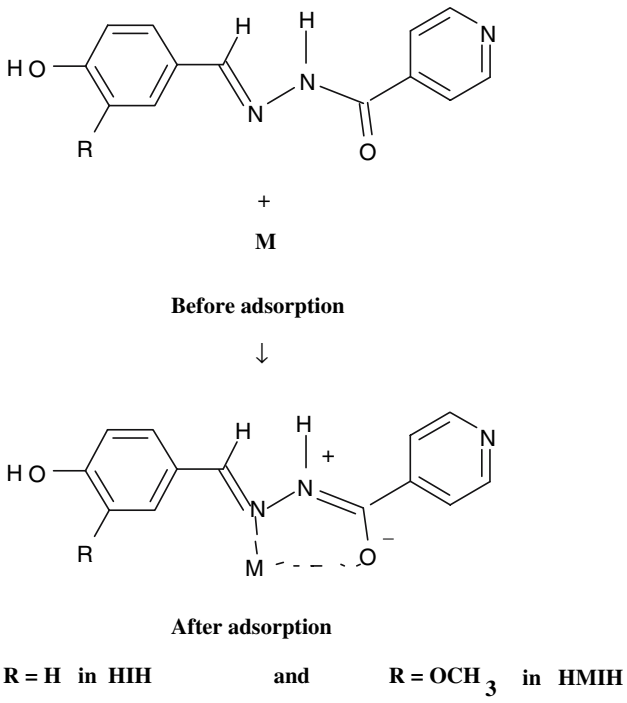

Fig. 8 Mechanism of adsorption of inhibitor molecules with the metal

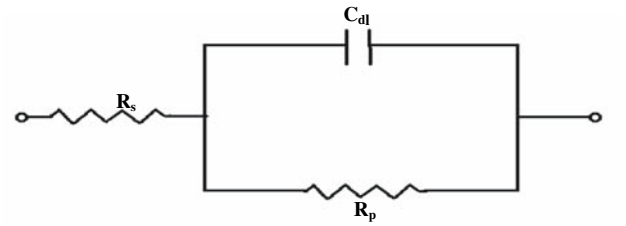

Fig. 9 Equivalent circuit for the metal–acid interface

and c show the micrographs after immersion in 1 M HCl containing HIH and HMIH, respectively. These SEM images show no signs of pits and corrosion products. This suggests that the inhibitors effectively control the corrosion process [30].

4 Conclusions

HIH and HMIH reduced the rate of corrosion of mild steel considerably in HCl. The IE% resulted from impedance, polarization and weight loss measurements were in good agreement. The HMIH containing an additional methoxy group exhibited higher corrosion inhibition efficiency. The rate of corrosion decreased with inhibitor concentration

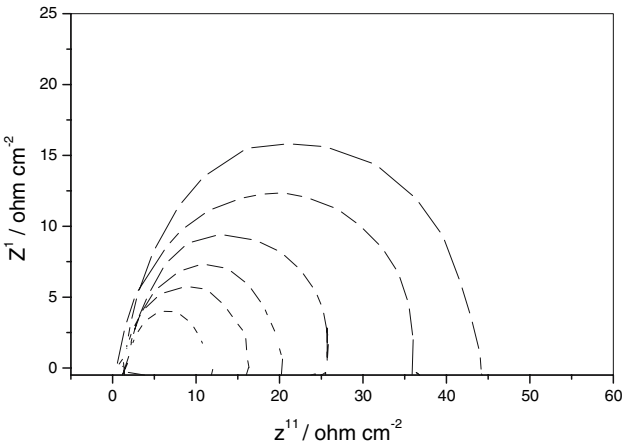

Fig. 10 Nyquist plots for mild steel in 1 M HCl in the absence and presence of different concentrations of HIH (1) Blank (2) 1.56×10^{-5} M (3) 3.13×10^{-5} M (4) 6.25×10^{-5} M (5) 12.5×10^{-5} M (6) 25×10^{-5} M

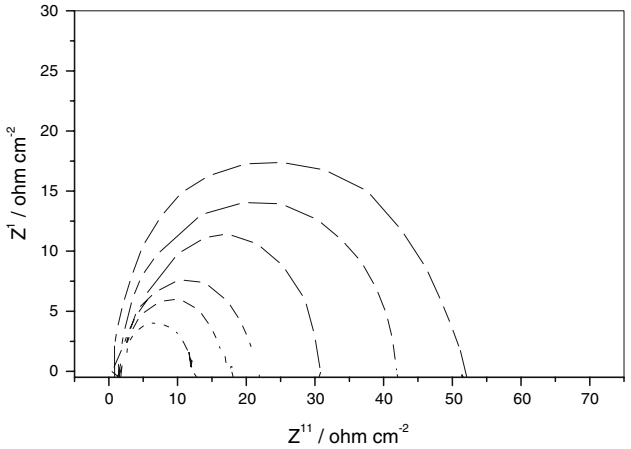

Fig. 11 Nyquist plots for mild steel in 1 M HCl in the absence and presence of different concentrations of HMIH (1) Blank (2) 1.56×10^{-5} M (3) 3.125×10^{-5} M (4) 6.25×10^{-5} M (5) 12.5×10^{-5} M (6) 25×10^{-5} M

Table 5 Electrochemical impedance parameters for mild steel in 1 M HCl in the presence and absence of inhibitors at different concentrations at 303 K

Inhibitor	Concentration ($10^5 \times$ M)	R_s (ohm)	R_p (ohm)	$10^5 \times$ CPE (F cm^2 S^{n-1})	n	IE (%)
–	0	1.70	12.8	5.65	0.863	–
HIH	1.56	2.01	17.4	6.84	0.87	26
	3.13	1.73	21.9	5.86	0.872	42
	6.25	1.51	26.5	4.71	0.841	52
	12.50	1.54	39.4	3.07	0.816	68
	25.00	1.50	45.5	2.13	0.762	72
HMIH	1.56	1.75	17.3	4.35	0.786	26
	3.13	1.71	22.9	3.68	0.79	44
	6.25	1.85	30.0	2.38	0.708	58
	12.50	1.72	43.7	1.24	0.715	71
	25.00	1.74	54.6	0.90	0.689	77

and increased with temperature. The data revealed that the inhibition action of tested compounds was through adsorption. The adsorption process obeyed the Langmuir adsorption isotherm. The thermodynamic data indicated spontaneous adsorption of inhibitor molecules. IR spectra revealed the interaction between inhibitor molecules and metal surface. SEM images of steel specimens in the presence of inhibitors showed an almost smooth surface indicating the protective action of the inhibitor. These results show that HIH and HMIH are good corrosion inhibitors for mild steel in HCl.

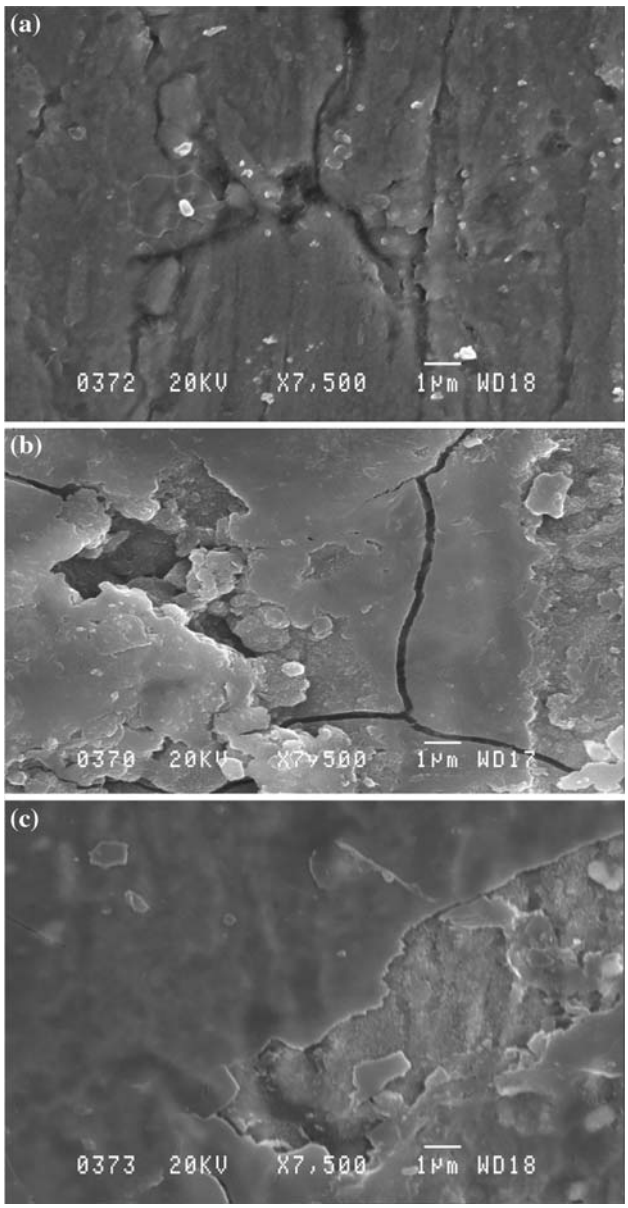

Fig. 12 (**a**) SEM Micrographs of mild steel surface in 1 M HCl. (**b**) SEM Micrographs of mild steel surface in 1 M HCl with HIH. (**c**) SEM Micrographs of mild steel surface in 1 M HCl with HMIH

References

1. Trabanelli G (1991) Corrosion 47:410
2. Raicheva SN, Aleksiev BV, Sokolova EI (1993) Corros Sci 34:343
3. Arab S, Noor EA (1993) Corrosion 49(2):122
4. Quraishi MA, Wajidkham MA, Ajmal M (1995) Bull Electrochem 11(6):274
5. Singh A, Choudhary RS (1996) Br Corros J 31(4):300
6. Abd El-Rehim SS, Ibrahim MAM, Khalid KF (1999) J Appl Electrochem 29:593
7. Quraishi MA, Sardar R, Jamal O (2001) Mater Chem Phys 71(3):309

8. Yurt A, Balaban A, Ustin Kandemiv S, Bereket G, Erx B (2004) Mater Chem Phys 85(2–3):420
9. Ashassi-Sorkhabi H, Shaabani B, Seifzadeh D (2005) Appl Surf Sci 239(2):154
10. Bentiss F, Traisnel M, Chaibi N, Mernari B, Vezin H, Lagrenee M (2002) Corros Sci 44:2271
11. Abd El-Rehim SS, Refaey SAM, Taha F, Saleh MB, Ahmed RA (2001) J Appl Electrochem 31:429
12. Tamil Selvi S, Raman V, Rajendran N (2003) J Appl Electrochem 33:1175
13. Khamis E (1990) Corrosion 46:476
14. Stupnisek-Lisac E, Metikos-Hukovia M (1993) Br Corros J 28:74
15. Stupnisek-Lisac E, Podbrscek S (1994) J Appl Electrochem 24:779
16. Bentiss F, Lagrenee M, Traisnel M, Hornez JC (1999) Corrosion 55:968
17. Raghavan PV (2000) Expert consultant. CPCSEA, OECD, guideline No. 420
18. Sathi G (1981) PhD work, Lucknow
19. Cronyn J.M. (1990) The elements of archaeological conservation. Routeledge, London
20. Bentiss F, Lagrenee M, Traisnel M, Hornez JC (1999) Corros Sci 41:789
21. Putilova IN, Balezin SA, Barannic VP, Bal T (1962) Corros Sci 2:22
22. Prabhu RA, Shanbhag AV, Venkatesha TV (2007) J Appl Electrochem 39:491
23. Gomma MK, Wahdan MH (1995) Mater Chem Phys 39:209
24. Savithri BV, Mayanna S (1996) Ind J Chem Technol 3:256
25. Chaudhary RS, Sharma S (1999) Ind J Chem Technol 6:202
26. Abdallah M (2002) Corros Sci 44:717
27. Mansfeld F (1982) Corrosion 38:570
28. Emregul Kaan C, Abdulkadir Akay A, Atakol O (2005) Mater Chem Phys 93:325
29. Muralidharan S, Chandrasekar R, Iyer SVK (2000) Proc Indian Acad Sci 112(2):127
30. Sahin M, Bigic S, Yilmaz H (2002) Appl Surf Sci 195:1